UDC 546.171.1/.718:539.89

Z. L. Zhao, K. Bao, D. F. Duan, X. L. Jin, F. B. Tian, D. Li, B. B. Liu, T. Cui*(Changchun, P. R. China)
**cuitian@jlu.edu.cn*

Ideal stoichiometric technetium nitrides under pressure: a first-principles study

Technetium nitrides with various ideal stoichiometries have been investigated with the first-principle method at the pressures between 0–60 GPa. It have been found that there could be many stable technetium nitrides including Tc_3N, Tc_2N, TcN, Tc_2N_3, TcN_2, TcN_3, and TcN_4, among which Tc_3N and Tc_2N subnitrides are synthesizable at zero pressure and could be applied to nuclear waste management, such as separate radioactive ^{99}Tc from nuclear fuel cycle. Moreover, N-rich TcN_3 and TcN_4 exhibit remarkable bulk properties and can be potential ultrastiff and hard materials.

***Keywords**: technetium nitride, crystal structure prediction, ultra-incompressible and hard materials, thermodynamic stability, dynamic stability.*

INTRODUCTION

Technetium nitrides are interested for two main reasons. One is that the combination of transition metals (TM) with light covalent-bond forming elements like B, C, and N might bring novel superhard materials [1]. The successful synthesis of platinum metals (PM) nitrides, such as PtN_2 [2, 3], IrN_2 [3, 4], OsN_2 [4], PdN_2 [5], and rhenium nitrides Re_3N, Re_2N [6], with high incompressibility under high pressure and high temperature (HPHT) gave the primary interest to explore the nitrides of 4*d* and 5*d* transition metals. Since technetium is adjacent to the platinum metals in the periodic table, the combination of technetium and nitrogen may pose new hard materials. The other is that although there is no stable isotopes of technetium, its long-lived isotope ^{99}Tc (half-life $t_{1/2}$ = 211,000 years) as a product of the nuclear fuel cycle constitutes an important challenge for environment remediation [7]. Therefore, the formation of stable Tc nitrides (especially of Tc-rich phases) with high chemical stability and corrosion resistance are important for the nuclear waste management.

In 1964, Tc nitride was firstly synthesized by Trzebiatowski and Rudzinski [8] by hydrogen reduction of NH_4TcO_4 in ammonia at 900–1100 °C or by thermal decomposition of $(NH_4)_2[TcCl_6]$ or $(NH_4)_2[TcBr_6]$ at 380 °C under argon atmosphere. The Tc–N phases were detected to crystallize in the face-center-cubic (fcc) structure with a varying lattice constant depending on the amount of nitrogen absorbed from 3.980 to 3.985 Å, and with a maximum nitrogen content approximated to the composition of $TcN_{0.76}$ [8]. Theoretically, Liang et al. [9] addressed the mechanical properties of hypothetical WC-type, NiAs-type, NaCl-type, and ZnS-type Tc monocarbide and mononitride with series first-principle calculations. They proposed that the WC-type and NiAs-type TcC and TcN are hard and ultrastiff materials. Most recently, Wang et al. [10] investigated 10 candidate structures for Tc mononitride and indicated that NiAs-type and NbO-type TcN are more energetically preferred. Recently, Tc subnitrides (Tc_3N and Tc_2N) based on the structures of Re subnitrides were also studied theoretically by Weck et al. [11]

and Do et al. [12]. However, compound can actually embody complex mixture ratios depending on the synthetic pathways, and previously investigated ratios of Tc nitrides (Tc_3N, Tc_2N, and TcN) were insufficient for providing a comprehensive reference to experimental synthesis and physical applications, while the structure searching methodology, such as USPEX code [13–15] might be a good answer to this problem, for its great ability in searching possible structures only naming the elements in a compound.

In this work, comprehensive first-principle studies on the structure, stability, and physical properties of technetium nitrides were performed with Tc/N ratios, including Tc_3N, Tc_2N, TcN, Tc_2N_3, TcN_2, TcN_3, and TcN_4. The proposed stoichiometries were based on the known Re nitrides and common 4*d* or 5*d* TM compounds [6, 16]. We have updated a full-scale zero-temperature Tc–N phase diagram at moderate low pressures from 0 to 60 GPa, in favor of further high-pressure experimental synthesis. Besides, the guidance for Tc nitrides in physical and chemical applications was also proposed.

COMPUTATIONAL DETAILS

To determine the stable structures of potential Tc–N phases, ab initio evolutionary structure searches [13–15] are performed at Tc/N ratios of Tc_3N, Tc_2N, TcN, Tc_2N_3, TcN_2, TcN_3, and TcN_4. Structure predictions are mainly focused on different pressures of 0, 30, and 60 GPa with systems containing one to four formula units (f.u.) in the simulation cell. The initial cell-vector lengths, angles, and atomic positions were all chosen randomly. Each structure was fully relaxed to an energy minimum at different pressures with the Vienna ab initio simulation package (VASP) [17]. The projector augmented waves (PAW) method [18] within the generalized gradient approximation (GGA) of Perdew, Burke and Ernzerhof (PBE) [19] was used. Besides, considered that the local density approximation (LDA) [20] usually gave a better cell geometry, LDA was used to determine the equilibrium lattice constants and elastic properties. For technetium, the semicore states ($4p^6 5s^2 4d^5$) were treated as valence states. By performing accurate convergence tests, the plane-wave cutoff energy was taken as 520 eV and a k-mesh of $0.03 \times 2\pi$ Å^{-1} within the Monkhorst-Pack scheme was used to sample the Brillouin zone, which ensures the error bars of total energies less than 1 meV per atom. Phonon curves were achieved by PHONOPY code [21, 22], which is a phonon analyzer based on the supercell approach [23] that involves the calculation of force constants from forces on atoms with finite displacements. Elastic constants were calculated by the strain-stress method, while bulk and shear moduli were derived from the Voigt-Reuss-Hill averaging scheme [24].

RESULTS AND DISCUSSION

Crystal structures determination

A rich phase diagram of Tc nitrides toward different Tc/N ratios is updated in this work. For Tc subnitrides, evolutionary algorithm confirmed that the structures of Tc_3N and Tc_2N are isomorphic to Re_3N and Re_2N, which form in hexagonal structure within space groups (SG) $P\bar{6}m2$ and $P6_3/mmc$, respectively. This result is consistent with the conclusions of Weck et al. [11] and Do et al. [12] that Tc subnitrides following the structures of Re subnitrides can be stable. For N-rich Tc nitrides, the proposed stable structures of Tc nitrides are schematically showed in Fig. 1. It follows that as the proportion of nitrogen increases, the crystal configure-

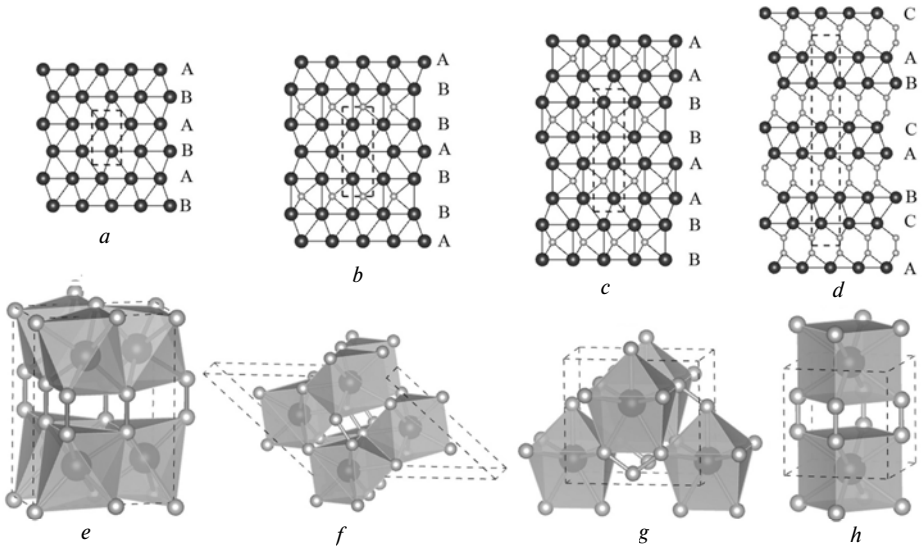

Fig. 1. Crystal structures of Tc nitrides, large balls represent Tc atoms, while small balls represent N atoms; (*a*, *b*, *c*) Crystal structures of Tc (SG $P6_3/mmc$), Tc_3N ($P\bar{6}m2$), and Tc_2N (SG $P6_3/mmc$), respectively; (*d*) hexa-TcN (SG $R\bar{3}m$): six f.u. per cell with Tc occupying the Wyckoff 6c (0, 0, 0.2278) sites, N occupying the 6c (0, 0, 0.9639); (*e*) orth-Tc_2N_3 (SG $Pmn2_1$): five f.u. per cell with Tc1 occupying the 2a (0.5, 0.2065, 0.1347), Tc2 occupying the 2a (0, 0.2130, 0.6923), N1 occupying the 2a (0.5, 0.4156, 0.8374), N2 occupy the 2a (0, 0.3818, 0.3374), and N3 occupying the 2a (0, 0.9755, 0.9859); (*f*) mono-TcN_2 (SG $C2/m$): four f.u. per cell with Tc occupying the 4i (0.9479, 0, 0.7704), N1 occupying the 4i (0.1275, 0, 0.5305), and N2 occupying the 4i (0.7398, 0, 0.8648), with $\beta = 137.7°$; (*g*) orth-TcN_3 (SG $Imm2$): two f.u. per cell, Tc atoms occupy the 2b (0.5, 0, 0.3471), N1 occupying the 4c (0.2107, 0.5, 0.2450), N2 occupying the 2b (0, 0.5, 0.4128); (h) tetr-TcN_4 (SG $P4/mmm$): only one f.u. per cell with Tc occupying the 1c (0.5, 0.5, 0), N occupying the 4i (0, 0.5, 0.3340).

tions transform from Tc–N lamellar structures (when the atomic fraction of N is less than or equal to 0.5, e.g., Tc_3N, Tc_2N, and TcN) to polyhedron stacking structures (when the atomic fraction of N is larger than 0.5, e.g., Tc_2N_3, TcN_2, TcN_3, and TcN_4). The structures of proposed TcN, TcN_2, and TcN_4 form in an *ABC* Tc lamellar stacking sequence with vertical N–N units connecting each two Tc layers, stacking of the corner or edge shared TcN_7 decahedron, and simple quadrangular prism stacking sequence, respectively (see Figs. 1, *d*, *f*, and *h*). For Tc_2N_3, a new orthorhombic structure (SG $Pmn2_1$) was achieved by evolutionary algorithm, as shown in Fig. 1, *e*. In the structure, the metal atoms were packaged by N atoms form a stacking of the corner or edge shared TcN_6 heptahedron and with vertical N–N bonds connecting each polyhedron layers. By increasing the nitrogen content in evolutionary algorithm, we get another orthorhombic phase within the space group $Imm2$ for TcN_3. In this structure, a Tc atom forms in elongated body-centered cubic lattice and the special three-nitrogen units can be formed in the (010) plane of crystal, which is apparently different from the common double N–N units in other N-rich nitrides. Actually, this structure can also be viewed as a polyhedron stacking structure as shown in Fig. 1, *g*. In the crystal, a Tc atom surrounded by every seven N atoms forms a TcN_7 octahedron and the adjacent polyhedron was connected by three-nitrogen units. The common stacking of polyhedral structures and strong N–N connections will be beneficial to the mechanical strength due to the three dimensional covalent network driven by directional hybridization of Tc*d* electrons and N*s*, *p* electrons can effectively

restrain the non-directional metallic bonds in Tc nitrides. The calculated lattice parameters, cell volume, and N–N bond–length were listed in Table 1. Our calculated lattice parameters are in good accordance with the earlier studies [11, 12], proving the reliability of our calculations.

Table 1. The calculated lattice constants *a*, *b*, *c*, cell volume per formula unit V_0, bulk modulus *B*, shear modulus *G*, Young's modulus *E*, Poisson's ratio *v*, Pugh's indicator *G*/*B*, and Vickers hardness H_V of Tc and Tc nitrides with various stoichiometries compared with available data

Phase	SG	*a*, Å	*b*, Å	*c*, Å	V_0, Å^3	*B*, GPa	*G*, GPa	*E*, GPa	*v*	*G*/*B*	H_V, GPa
Tc	$P6_3/mmc$	2.72		4.35	27.87	343	165	427	0.29	0.48	14.9
		2.74[a]		4.40[a]							
Tc_3N	$P\bar{6}m2$	2.78		6.99	46.80	379	202	514	0.27	0.53	19.3
		2.83[b]		7.08[b]							
		2.82[c]		7.08[c]							
Tc_2N	$P6_3/mmc$	2.80		9.66	32.79	390	185	480	0.29	0.48	16.0
		2.85[b]		9.75[b]							
		2.84[c]		9.75[c]							
TcN	$R\bar{3}m$	2.79		18.12	20.31	362	187	479	0.28	0.52	17.7
Tc_2N_3	$Pmn2_1$	2.78	6.59	5.00	45.84	386	194	499	0.28	0.50	17.6
TcN_2	$C2/m$	6.68	2.83	8.31	26.42	372	174	452	0.30	0.47	15.0
TcN_3	$Imm2$	5.16	2.76	4.67	33.29	334	229	560	0.22	0.69	28.2
TcN_4	$P4/mmm$	3.53		3.61	44.90	231	157	384	0.22	0.68	21.2

Sources: [a][25], [b][11], [c][12]

Thermodynamic and dynamic stability

Thermodynamic stability of materials can be estimated from the formation enthalpy, which is a good approximation of the zero-temperature phase diagram. The convex hull is defined as an average atom enthalpy versus the proportions of nitrogen plot with a set of lines connecting the low energy structures. Thus, convex hull is suited for determining the possible stable phases toward different stoichiometries. In principle, structures with an enthalpy on the convex hull is considered to be thermodynamically stable and synthesizable within experiment. The details of the formation enthalpy calculations have been described elsewhere [25]. Figure 2 presents the calculated convex hulls for Tc–N system at different pressures. First, we note that both Tc_3N and Tc_2N subnitrides are thermodynamically stable toward the whole considered pressures due to the fact that the formation enthalpy is on the convex hulls consistently, which means that Tc subnitrides can be formed by Tc integrate with nitrogen at ambient pressure. As mentioned above, although Tc possesses no stable isotopes, its long-lived isotope ^{99}Tc is produced in sizeable amounts from the nuclear fuel cycle. To manage the radioactive ^{99}Tc, pursuit of forming Tc nitrides, especially in Tc-rich Tc–N phases, is a viable approach. The formation of stable Tc_3N and Tc_2N subnitrides at ambient conditions will support their applications in this field. For Tc mononitrides, the proposed hexagonal TcN (SG $R\bar{3}m$) is more stable than previous NiAs-type and NbO-type TcN at low pressures (less than 40 GPa). NiAs-type TcN can be thermodynamically stable at elevated pressures and finally become the most stable

phase for TcN at a pressure more than 40 GPa. It follows from Fig. 2 that at the athermal limit, high pressure conditions are needed to the synthesis of N-rich Tc nitrides. We find that N-rich TcN, Tc_2N_3, TcN_2, and TcN_3 are thermodynamically stable and synthesizable within experiment at a pressure more than 20 GPa. Besides, there is a shift of the lowest enthalpy toward pressures, following the sequence: Tc_3N (0 GPa) → Tc_2N (10 GPa) → TcN (20–30 GPa) → Tc_2N_3 (beyond 30 GPa). The shift of the lowest enthalpy with pressures indicates the diversity of Tc–N phases, and appeals the significance of pressure effect on designing and searching new materials.

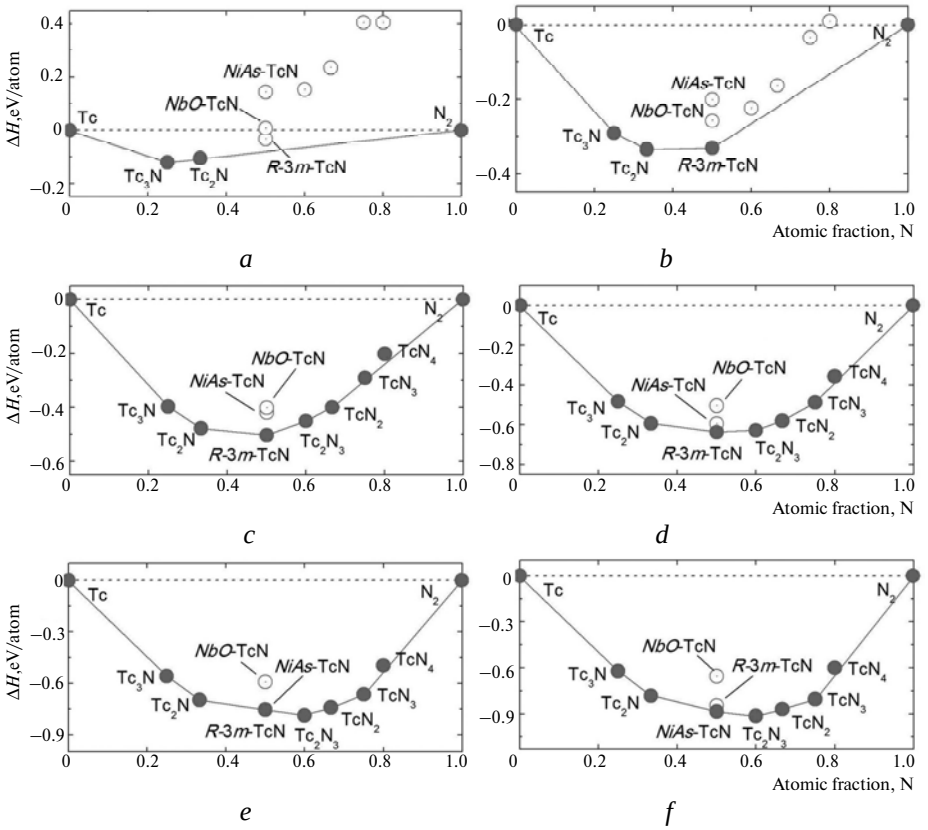

Fig. 2. Convex hulls for Tc–N system at pressures of (*a*) 0, (*b*) 10, (*c*) 20, (*d*) 30, (*e*) 40, and (*f*) 50 GPa.

It is well known that phonon studies give crucial information about global structural stability of materials. To test the lattice stability of the proposed Tc–N phases, we analyze both of the phonon spectra and partial phonon density of states (PPHDOS) to allow for possible soft phonon modes at low-symmetry points of the Brillouin zone (BZ), shown in Fig. 3 and Fig. 4. The calculated phonon curves and PPHDOS of proposed Tc_3N, Tc_2N, TcN, TcN_2, TcN_3, and TcN_4 have no soft mode in the BZ at zero pressure, indicating that they are all dynamically stable. Note that the dynamical stability of N-rich nitrides (TcN, TcN_2, TcN_3, and TcN_4) at zero pressure is a powerful argument to confirm that they are all quenchable to ambient pressure. Although Tc_2N_3 is lattice unstable around Y and S point of the BZ at low pressures, pressures can stabilize Tc_2N_3 at approximate 30 GPa according to our detailed calculations. According to Fig. 4, an analogical appearance of the

PPHDOS was revealed. The main contribution to acoustic phonons results from the Tc sublattice, while the high-frequency phonons stems from the N atoms. Besides, a common strong N–N coupling existed in N-rich Tc nitrides, indicating covalent characters of the N–N bonds.

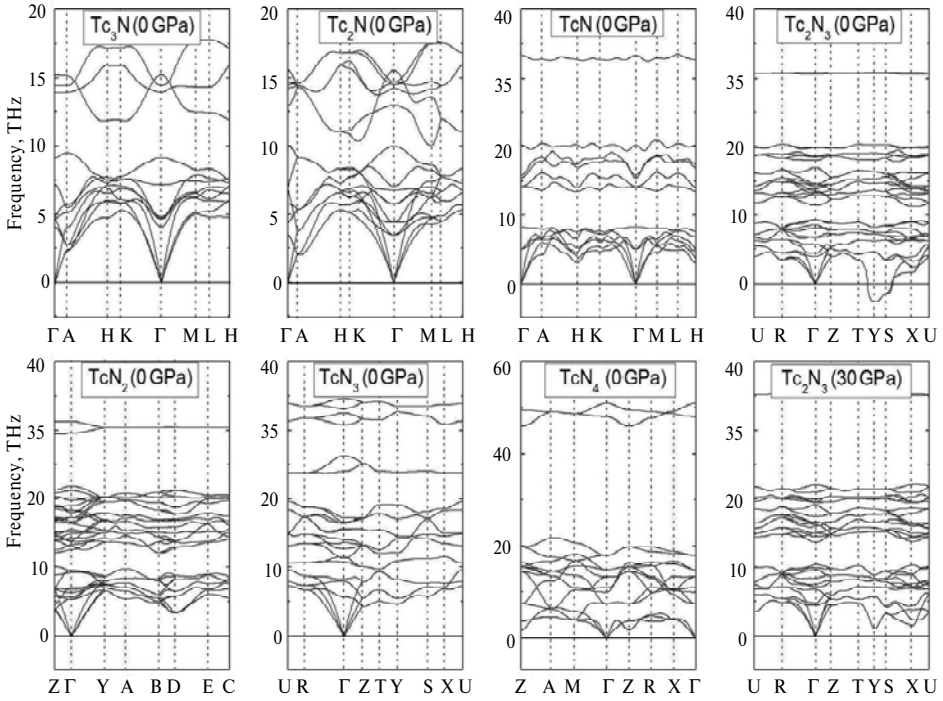

Fig. 3. Phonon dispersion curves for Tc_3N, Tc_2N, TcN, Tc_2N_3, TcN_2, TcN_3, and TcN_4 at different pressures.

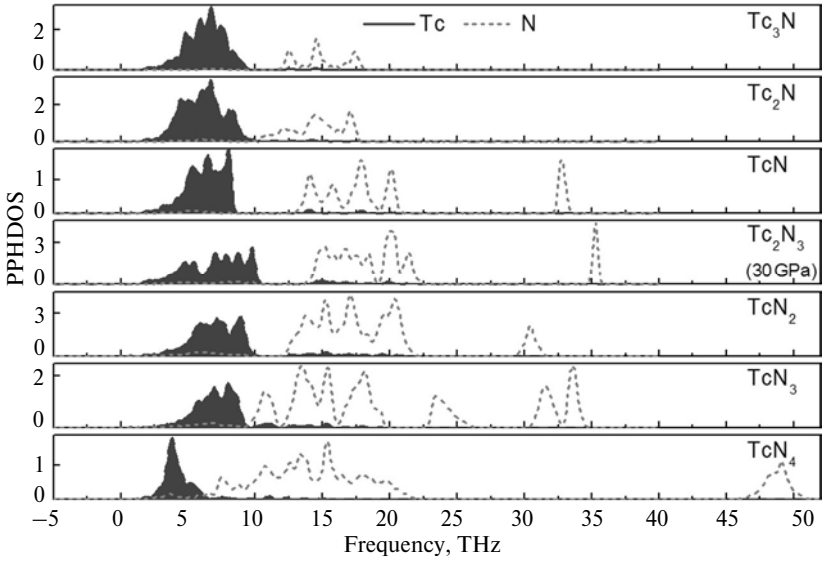

Fig. 4. Partial atomic phonon density of states (PPHDOS) for Tc_3N, Tc_2N, TcN, TcN_2, TcN_3, and TcN_4 at zero pressure, and for Tc_2N_3 at 30 GPa, respectively.

Elastic properties and electronic structure analysis

The calculated zero-pressure elastic constants of variously stoichiometric Tc nitrides are listed in Table 2. We have tested that all the elastic constants fulfill the Born-Huang stability criteria [26], indicating that they are all mechanically stable. For the proposed TcN (SG $R\bar{3}m$), we find a relative high incompressibility along the *c*-axis, as demonstrated by a larger C_{33} in Table 2. The high incompressibility of TcN along the *c*-axis can be attributed to the existence of the N–N bonds in this direction. In fact, the high N ratio induced strong N–N connections and polyhedron stacking structures in N-rich Tc nitrides produced much remarkable elastic properties. For example, N–N bonds along the *b*-axis in the crystal produce a much higher C_{22} for Tc_2N_3, N–N connections along the *c*-axis elevated the value of C_{33} nearly two times larger than C_{11} in TcN_4, and three-nitrogen units in (010) plane give the largest C_{11} and C_{33} for N-rich TcN_3 compared with other Tc nitrides. Large elastic constant in N-rich nitrides is a harbinger of ultrastiff material as discussed following.

Table 2. Calculated elastic constants C_{ij} (GPa) of Tc nitrides with various stoichiometries

Phase	C_{11}	C_{22}	C_{33}	C_{44}	C_{55}	C_{66}	C_{12}	C_{13}	C_{23}
Tc_3N	618		733	197		203	213	258	
Tc_2N	612		728	172		201	210	292	
TcN	563		738	192		173	217	248	
Tc_2N_3	580	828	542	217	160	234	240	226	337
TcN_2	823	529	636	127	232	142	229	251	237
TcN_3	889	484	772	140	274	239	215	193	89
TcN_4	356		694	163		138	105	144	

The calculated bulk and shear moduli, Young's modulus, Poisson's ratio, Pugh's indicator, and Vickers hardness are all listed in Table 1. It can be seen that large elastic modulus is a common character of Tc nitrides. Among them, Tc_3N, Tc_2N, Tc_2N_3, and TcN_2 exhibit remarkable bulk modulus close to 400 GPa, which indicates that they are all difficult to compress. However, the bulk modulus of Tc nitrides decreases, especially for N-rich TcN_3 and TcN_4, as the atomic fraction N is increased. This can be explained by the internal electronic structure changes induced by the increasing of nitrogen content. Figure 5 presents the calculated total and site projected electronic densities of states (PDOS) of Tc nitrides. All the proposed Tc–N phases have similar metallic bonding features owing to finite DOS at the Fermi level (E_F), which originate mostly from the 4*d* electrons of Tc. It is worth noting that there is a strong hybridization between N 2*p* and Tc 4*d* states responsible for the formation of covalent Tc–N bonds. As the atomic fraction N increases, more powerful hybridization between N 2*p* and Tc 4*d* states in N-rich Tc nitrides compared with subnitrides was revealed. The enhanced orbital hybridization results in strong covalent bonding in N-rich Tc nitrides, and causes the significant decrease of free electrons density. It is well known that bulk modulus is closely related to the valence electron density (VED) because higher concentrations of electrons result in greater repulsive forces within the material [27]. Reasonably, the reduced valence electron density and increased covalent bonding lower the bulk modulus of N-rich Tc nitrides toward subnitrides. In turn, however, strong covalent bonding in N-rich Tc nitrides means a high level of ma-

terials resistance to plastic deformations. As a result, although with a low bulk modulus, N-rich TcN_3 exhibits the largest shear modulus (229 GPa) and Young's modulus (560 GPa) among all proposed Tc nitrides according to Table 1. Besides, TcN_3 and TcN_4 possess the minimum of the Poisson's ratio (0.22 and 0.23) and the maximum of Pugh's indicator *G/B* (0.69 and 0.66), suggesting that both of them are brittle and hard materials with a high capability to resist elastic-plastic deformations. Most recently, Chen et al. [28] have proposed a model of hardness by the Pugh's modulus ratio, $k = G/B$, which correlated both the elasticity and plasticity of materials. The Vickers hardness can be calculated as $H_V = 2(k^2G)^{0.585} - 3$. Note that this formula predicts the hardness of materials that fairly well agrees with experimental data. Herein, the Vickers hardness of Tc–N phase was calculated and listed in Table 1. The calculated hardness for TcN_3 and TcN_4 are of 28.2 and 20.0 GPa, respectively, which match hard materials of WC (21.5–33.4 GPa) [28–30]. Our results suggest that N-rich TcN_3 and TcN_4 can be potential candidate to be ultrastiff and hard materials.

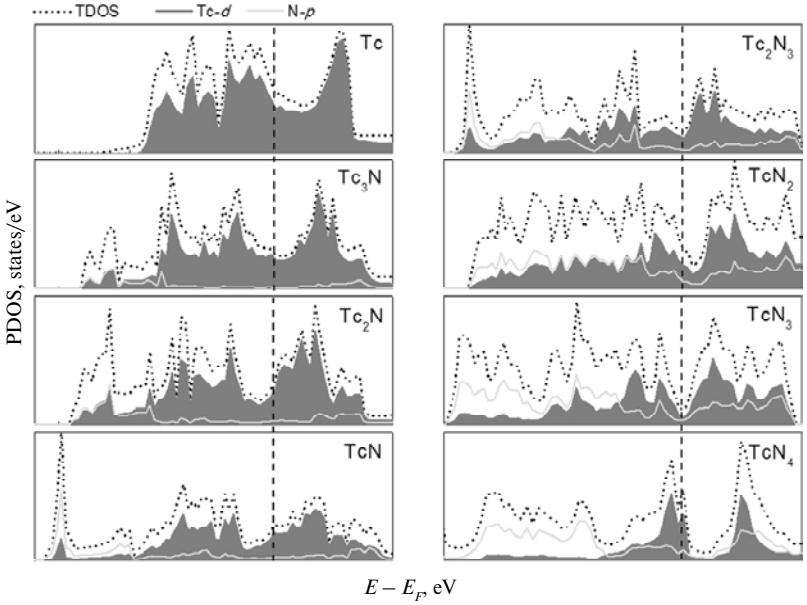

Fig. 5. Total (TDOS) and partial density of states (PDOS) for Tc–N system at 0 GPa. The vertical dashed line at zero is the Fermi energy level.

CONCLUSIONS

We have updated a full-scale zero-temperature Tc–N phase diagram by a series of first principle calculations. We find that Tc_3N and Tc_2N subnitrides can be synthesized at ambient condition and support their applications in nuclear waste management, while all the N-rich Tc nitrides are synthesizable in experiments at moderate pressures about 20 GPa. A common high incompressibility of Tc nitrides is revealed, and N-rich TcN_3 and TcN_4 can be potential candidate for ultrastiff and hard materials with the Vickers hardness comparable to hard WC.

This work was supported by the National Basic Research Program of China (No. 2011CB808200), Program for Changjiang Scholars and Innovative Research Team in University (No. IRT1132), National Natural Science Foundation of China (Nos. 51032001, 11074090, 10979001, 51025206), and National Found for Foster-

ing Talents of basic Science (No. J1103202). Parts of calculations were performed in the High Performance Computing Center (HPCC) of Jilin University.

Нітриди технеція з різною ідеальної стехіометрією досліджені із застосуванням методу перших принципів при тисках від 0 до 60 ГПа. Встановлено, що може бути багато стабільних нітридів технеція, включаючи Tc_3N, Tc_2N, ТКС, Tc_2N_3, TcN_2, TcN_3 і TcN_4, серед яких субнітриди Tc_3N і Tc_2N синтезуються при нульовому тиску і можуть бути використані для обробки ядерних відходів, таких як виділений при ядерному паливному циклі радіоактивний ^{99}Tc. Більш того, TcN_3 і TcN_4, збагачені N, демонструють чудові об'ємні властивості і можуть бути потенційними ультражорсткими і твердими матеріалами.

***Ключові слова**: нітрид технеція, прогнозування кристалічної структури, ультранестискувані і тверді матеріали, термодинамічна стабільність, динамічна стабільність.*

Нитриды технеция с различной идеальной стехиометрией исследованы с применением метода первых принципов при давлениях от 0 до 60 ГПа. Установлено, что может быть много стабильных нитридов технеция, включая Tc_3N, Tc_2N, ТКС, Tc_2N_3, TcN_2, TcN_3 и TcN_4, среди которых субнитриды Tc_3N и Tc_2N синтезируются при нулевом давлении и могут быть использованы для обработки ядерных отходов, таких как выделенный при ядерном топливном цикле радиоактивный ^{99}Tc. Более того, TcN_3 и TcN_4, обогащенные N, демонстрируют замечательные объемные свойства и могут быть потенциальными ультражесткими и твердыми материалами.

***Ключевые слова**: нитрид технеция, прогнозирование кристаллической структуры, ультранесжимаемые и твердые материалы, термодинамическая стабильность, динамическая стабильность.*

1. *Kaner R. B., Gilman J. J., Tolbert S. H.* Designing superhard materials // Science. – 2005. – **308**. – P. 1268–1269.
2. *Gregoryanz E., Sanloup C., Somayazulu M. et al.* Synthesis and characterization of a binary noble metal nitride // Nat. Mater. – 2004. – **3**. – P. 294–297.
3. *Crowhurst J. C., Goncharov A. F., Sadigh B. et al.* Synthesis and characterization of the nitrides of platinum and iridium // Science. – 2006. – **311**. – P. 1275–1278.
4. *Young A. F., Sanloup C., Gregoryanz E. et al.* Synthesis of novel transition metal nitrides IrN_2 and OsN_2 // Phys. Rev. Lett. – 2006. – **96**, art. 155501.
5. *Crowhurst J. C., Goncharov A. F., Sadigh B. et al.* Synthesis and characterization of nitrides of iridium and palladium // J. Mater. Res. – 2008. – **23**. – P. 1–5.
6. *Friedrich A., Winkler B., Bayarjargal L. et al.* Novel rhenium nitrides // Phys. Rev. Lett. – 2010. – **105**, art. 085504.
7. *Maes A., Geraedts K., Bruggeman C. et al.* Evidence for the interaction of technetium colloids with humic substances by X-ray absorption spectroscopy // Environ. Sci. Technol. – 2004. – **38**. – P. 2044–2051.
8. *Trzebiatowski W., Rudzinski J.* The composition and structure of technetium nitride and technetium borides // J. Less Common Met. – 1964. – **6**. – P. 244–245.
9. *Liang Y., Li C., Guo W., Zhang W.* First-principles investigation of technetium carbides and nitrides // Phys. Rev. B. – 2009. – **79**, art. 024111.
10. *Wang Y., Yao T., Li H. et al.* Structural stability, phase transition, and mechanical and electronic properties of transition metal nitrides MN (M = Tc, Re, Os, and Ir): first-principles calculations // Comp. Mater. Sci. – 2012. – **56**. – P. 116–121.
11. *Weck P. F., Kim E., Czerwinski K. R.* Interplay between structure, stoichiometry, and properties of technetium nitrides // Dalton Trans. – 2011. – **40**. – P. 6738–6744.
12. *Du X. P., Lo V. C., Wang Y. X.* The effect of structure and phase transformation on the mechanical properties of Re_2N and the stability of Mn_2N // J. Comput. Chem. – 2012. – **33**. – P. 18–24.
13. *Oganov A. R., Glass C. W.* Crystal structure prediction using *ab initio* evolutionary techniques: Principles and applications // J. Chem. Phys. – 2006. – **124**, art. 244704.
14. *Oganov A. R., Lyakhov A. O., Valle M.* How evolutionary crystal structure prediction works–and why // Acc. Chem. Res. – 2011. – **44**. – P. 227–237.

15. *Lyakhov A. O., Oganov A. R., Stokes H. T., Zhu Q*. New developments in evolutionary structure prediction algorithm USPEX // Comput. Phys. Commun. – 2013. – **184**. – P. 1172–1182.
16. *Friedrich A., Winkler B., Juarez-Arellano E. A., Bayarjargal L.* Synthesis of binary transition metal nitrides, carbides and borides from the elements in the laser-heated diamond anvil cell and their structure-property relations // Materials. – 2011. – **4**. – P. 1648–1692.
17. *Kresse G., Furthmüller J.* Efficient iterative schemes for ab initio total-energy calculations using a plane-wave basis set // Phys. Rev. B. – 1996. – **54**. – P. 11169–11186.
18. *Kresse G., Joubert D.* From ultrasoft pseudopotentials to the projector augmented-wave method // Ibid. – 1999. – **59**. – P. 1758–1775.
19. *Perdew J. P., Burke K., Ernzerhof M.* Generalized gradient approximation made simple // Phys. Rev. Lett. – 1996. – **77**. – P. 3865–3868.
20. *Perdew J. P., Zunger A.* Self-interaction correction to density-functional approximations for many-electron systems // Phys. Rev. B. – 1981. – **23**. – P. 5048–5079.
21. *Togo A.* http://phonopy.sourceforge.net/
22. *Togo A., Oba F., Tanaka I.* First-principles calculations of the ferroelastic transition between rutile-type and $CaCl_2$-type SiO_2 at high pressures // Phys. Rev. B. – 2008. – **78**, art. 134106.
23. *Parlinski K., Li Z. Q., Kawazoe Y.* First-principles determination of the soft mode in cubic ZrO_2 // Phys. Rev. Lett. – 1997. – **78**. – P. 4063–4066.
24. *Hill R.* The elastic behavior of a crystalline aggregate // Proc. Phys. Soc. Sect. A. – 1952. – **65**. – P. 349–354.
25. *Li D., Tian F., Duan D. et al*. Mechanical and metallic properties of tantalum nitrides from first-principles calculations // RSC Adv. – 2014. – **4**. – P. 10133–10139.
26. *Wu Z. J., Zhao E. J., Xiang H. P. et al*. Crystal structures and elastic properties of superhard IrN_2 and IrN_3 from first principles // Phys. Rev. B. – 2007. – **76**, art. 054115.
27. *Gilman J. J., Cumberland R. W., Kaner R. B.* Design of hard crystals // Int. J. Refract. Met. Hard Mater. – 2006. – **24**. – P. 1–5.
28. *Chen X. Q., Niu H. Y., Li D. Z., Li Y. Y.* Modeling hardness of polycrystalline materials and bulk metallic glasses // Intermetallics. – 2011. – **19**. – P. 1275–1281.
29. *Gao F., He J., Wu E. et al*. Hardness of covalent crystals // Phys. Rev. Lett. – 2003. – **91**, art. 015502.
30. *Šimůnek A., Vackář J.* Hardness of covalent and ionic crystals: first-principle calculations // Ibid. – 2006. – **96**, art. 085501.

State Key Laboratory of Superhard Materials,
College of Physics, Jilin University, Changchun, P.R. China

Received 27.03.14